Science Advances

Supplementary Materials for

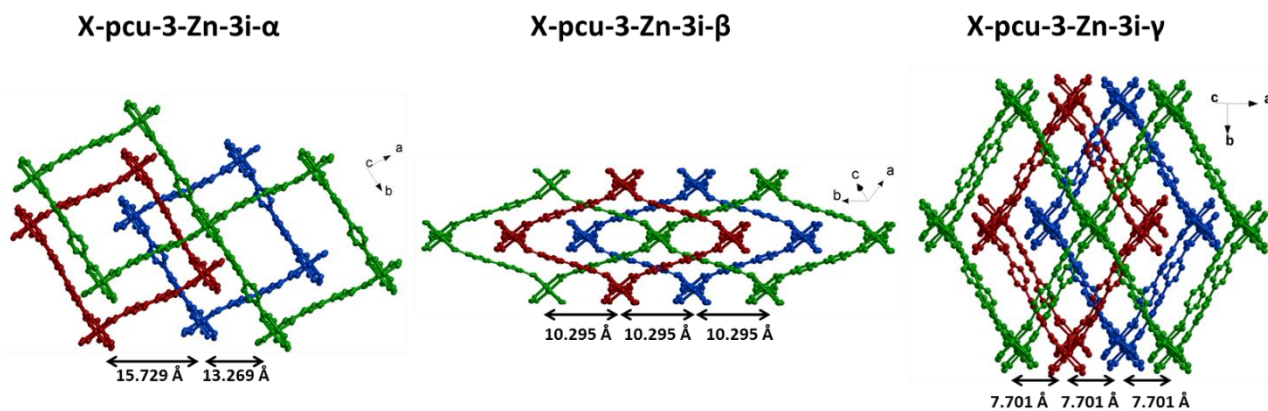### Readily accessible shape-memory effect in a porous interpenetrated coordination network

Mohana Shivanna, Qing-Yuan Yang, Alankriti Bajpai, Susan Sen, Nobuhiko Hosono, Shinpei Kusaka, Tony Pham, Katherine A. Forrest, Brian Space, Susumu Kitagawa, Michael J. Zaworotko
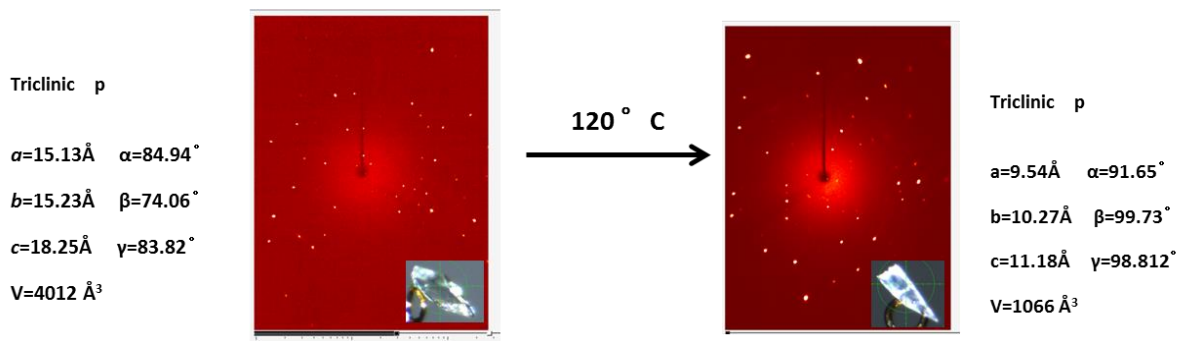
This PDF file includes:

- fig. S1. Structure of the three phases.
- fig. S2. Diffraction pattern and single-crystal images.
- fig. S3. Low-pressure gas sorption.
- fig. S4. Recyclability of shape-memory phase at 195 K CO_2.
- fig. S5. High-pressure CO_2 sorption.
- fig. S6. In situ variable temperature PXRD.
- fig. S7. Solvent-induced phase change.
- fig. S8. PXRD data for **X-pcu-3-Zn-3i-γ** obtained from different experiments.
- fig. S9. Phase change from γ to α phase.
- fig. S10. Variable temperature PXRD of shape-memory phase.
- fig. S11. Distortion of paddlewheel MBB and orientation of X-ligands in **X-pcu-3-Zn-3i-α**.
- fig. S12. Distortion of paddlewheel MBB and orientation of X ligands in **X-pcu-3-Zn-3i-β**.
- fig. S13. Distortion of paddlewheel MBB and orientation of X ligands in **X-pcu-3-Zn-3i-γ**.
- fig. S14. Thermogravimetric analysis (TGA) profiles.
- fig. S15. Comparison of modeling and experimental isotherm.
- fig. S16. Free-energy difference.
- fig. S17. Chemically distinct atoms in **X-pcu-3-Zn-3i-α**.
- fig. S18. The chemically distinct atoms in **X-pcu-3-Zn-3i-β**.
- fig. S19. The chemically distinct atoms in **X-pcu-3-Zn-3i-γ**.
- table S1. Examples of previously reported FMOMs with large hysteresis.
- table S2. Crystal data and refinement parameters.

fig. S1. Structure of the three phases. Relative orientation of the three interpenetrated networks in **X-pcu-3-Zn-3i** shown in red, blue and green.

In-situ Single Crystal-to-Single Crystal (SCSC) transformation studies

Triclinic   p

a=15.13Å   α=84.94°

b=15.23Å   β=74.06°

c=18.25Å   γ=83.82°

V=4012 Å³

120°C

Triclinic   p

a=9.54Å   α=91.65°

b=10.27Å   β=99.73°

c=11.18Å   γ=98.812°

V=1066 Å³

fig. S2. Diffraction pattern and single-crystal images. A single crystal undergoes transformation from **X-pcu-3-Zn-3i-α** to **X-pcu-3-Zn-3i-β** at 120 °C in SC-SC fashion.

Gas sorption studies
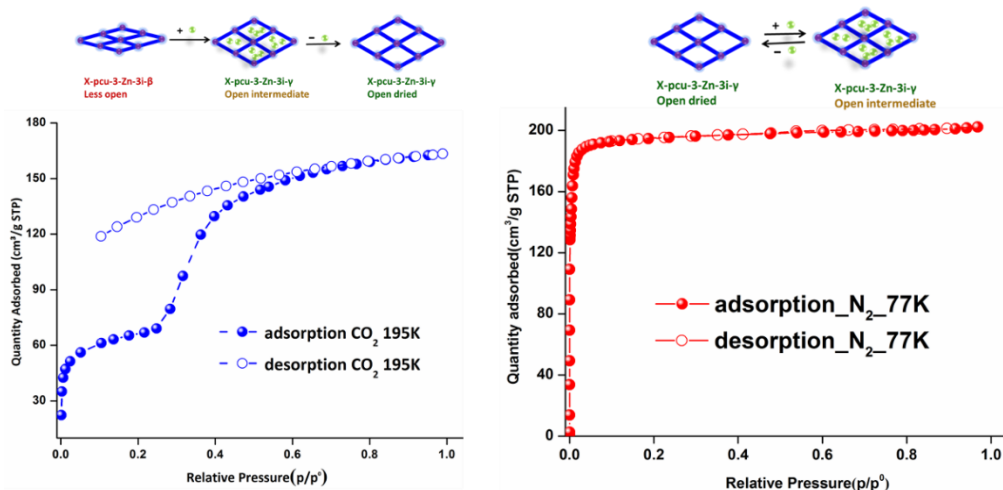
**fig. S3. Low-pressure gas sorption.** Low temperature gas sorption on **X-pcu-3-Zn-3i.** First cycle of **X-pcu-3-Zn-3i-β** exhibits stepped isotherm and then it transforms to shape memory phase, **X-pcu-3-Zn-3i-γ** followed of N_2 adsorption isotherms showed a type I profile. a) 195 K CO_2, adsorption (closed blue circles) and desorption (open blue circles), 77 K N_2, adsorption (closed red circles) and desorption (open red circles). The BET surface area (S_{BET}) of X-pcu-3-Zn-3i-γ, the S_{BET} was found to be 800 m^2g^{-1} calculated from 77 K N_2 sorption.
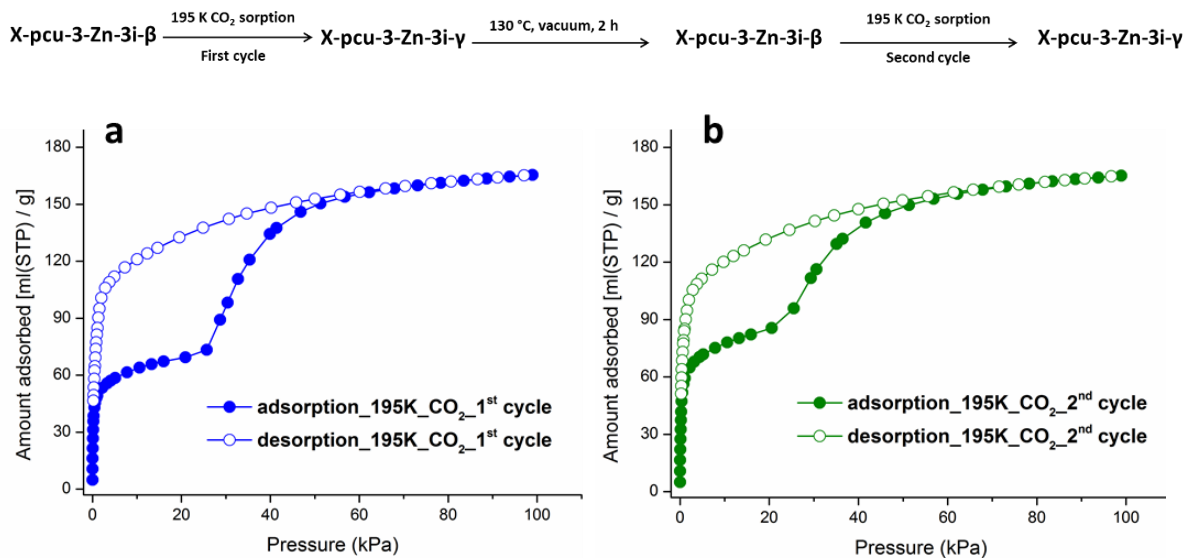
fig. S4. Recyclability of shape-memory phase at 195 K CO_2. (**A**) First cycle of 195 K CO_2 sorption. (**B**) Sample obtained after the first cycle was regenerated (130 °C, 2 h *in vacuo*) and second cycle of 195 K CO_2 sorption was measured**.**
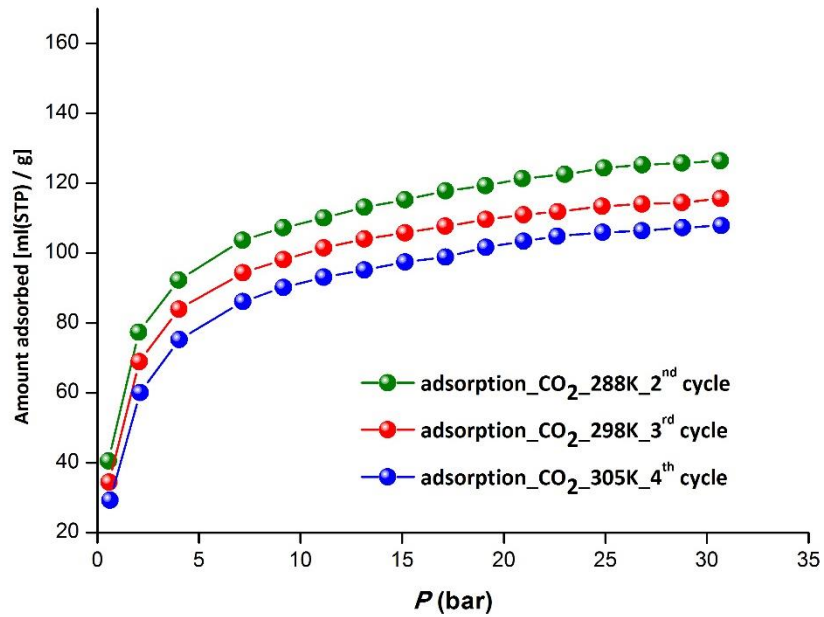
fig. S5. High-pressure CO₂ sorption. Three consecutive cycles at 288 K, 298 K and 305 K after first cycle**.**

In-situ variable temperature PXRD
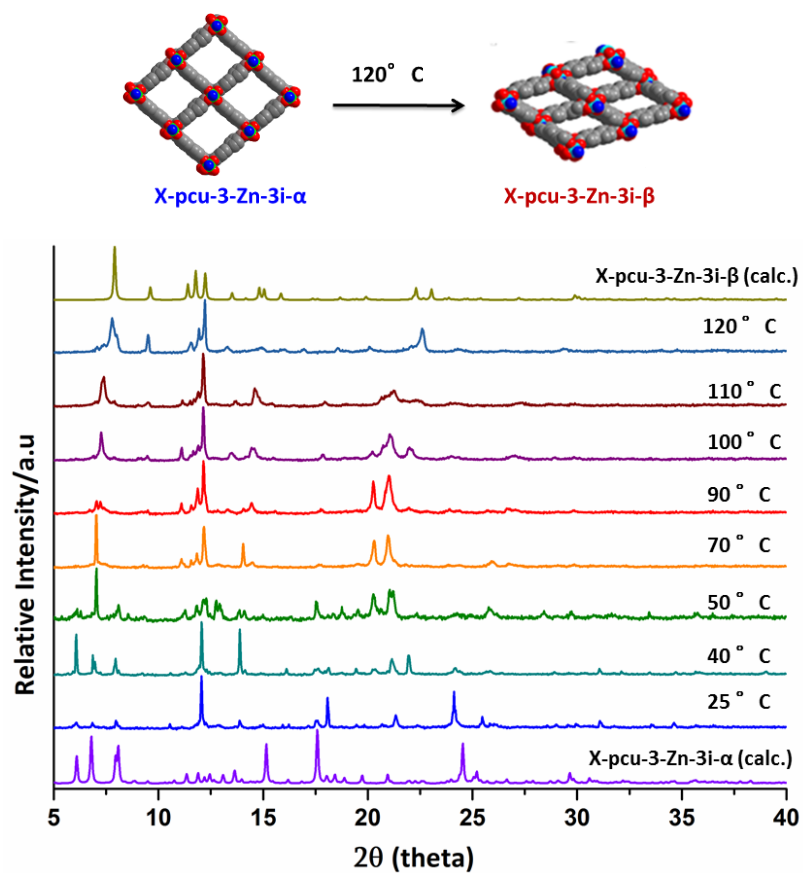
fig. S6. In situ variable temperature PXRD. X-pcu-3-Zn-3i-α undergoes phase transformation at 120 °C.

PXRD studies: interconversion of phases
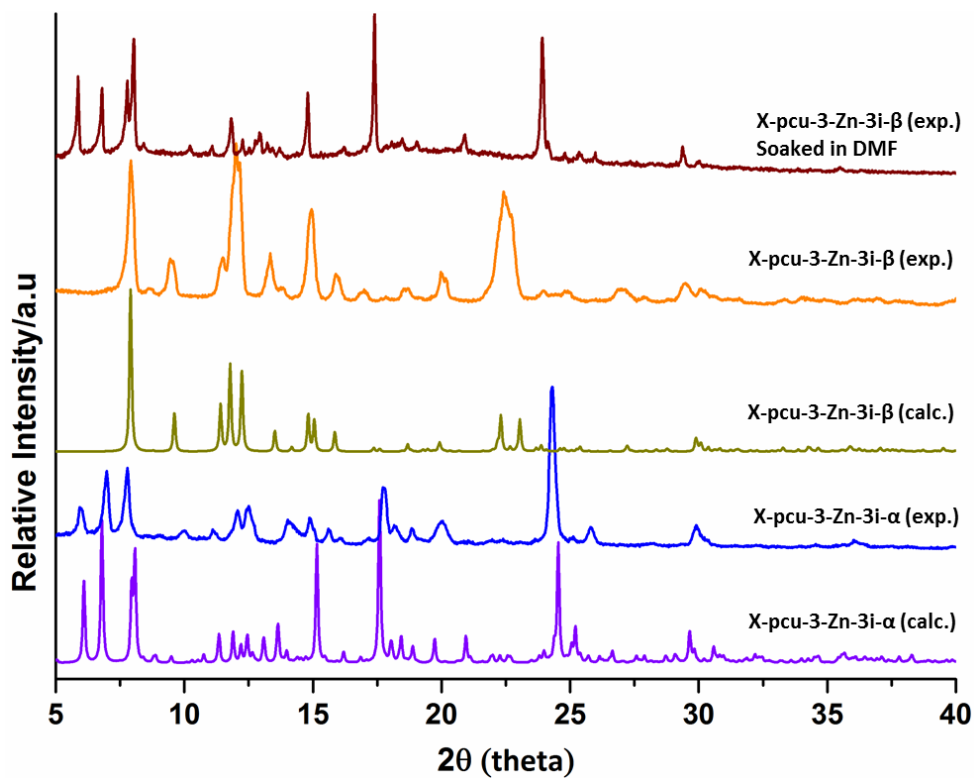
fig. S7. Solvent-induced phase change. PXRD: conversion of **X-pcu-3-Zn-3i-β** to **X-pcu-3-Zn-3i-α** after soaking in DMF.
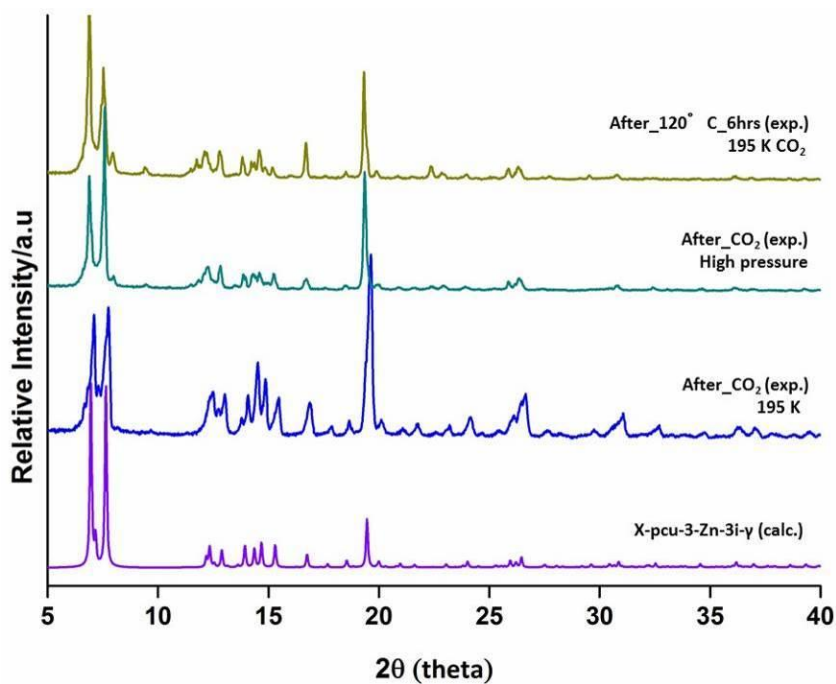
fig. S8. PXRD data for X-pcu-3-Zn-3i-γ obtained from different experiments.
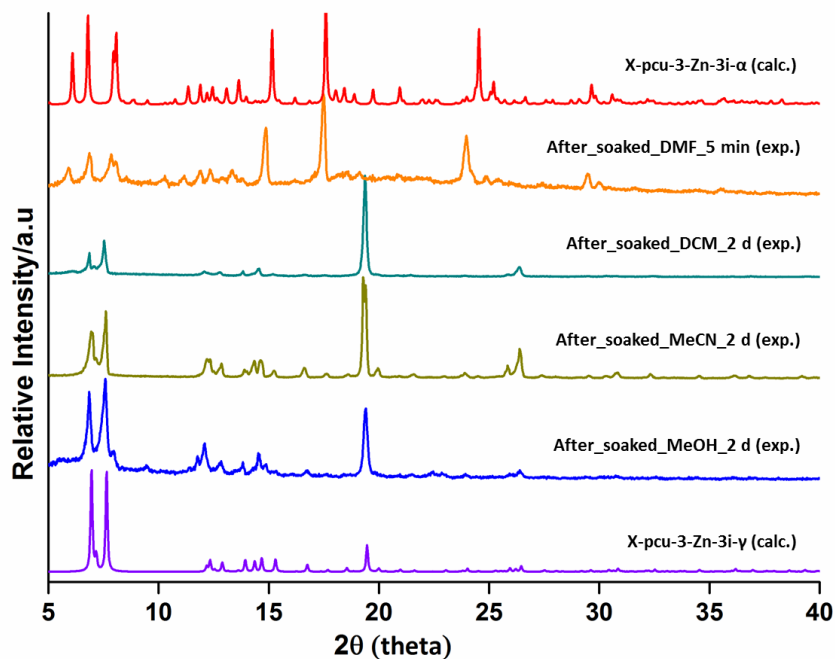
fig. S9. Phase change from γ to α phase. Comparison of PXRD patterns shows that **X-pcu-3-Zn-3i-γ** reverts to **X-pcu-3-Zn-3i-α** only in soaking in DMF.
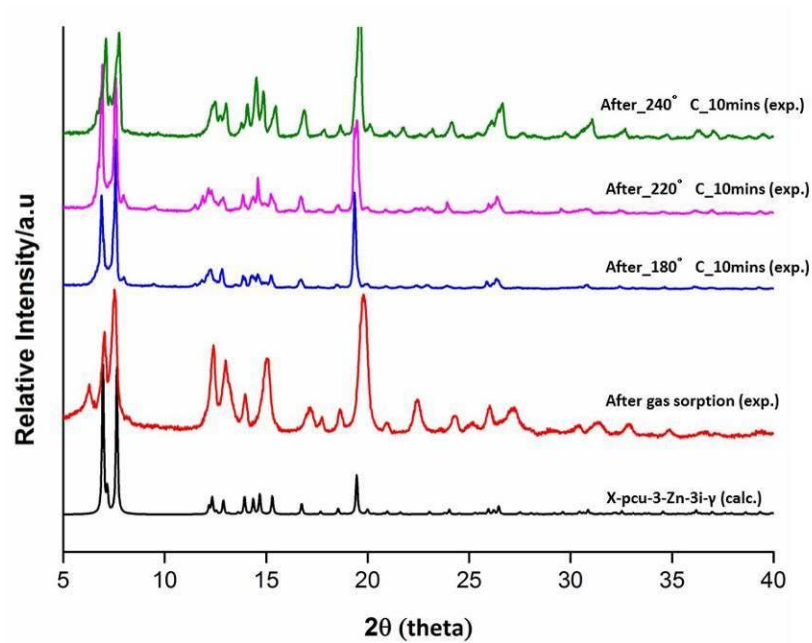
fig. S10. Variable temperature PXRD of shape-memory phase. PXRD patterns show that **X-pcu-3-Zn-3i-γ** retained on heating up to 240°C.

Distortion of paddlewheel MBB: bond angles

A centroid (C) was created for the paddlewheel MBB. Bond angles were measured for each linker through this centroid.
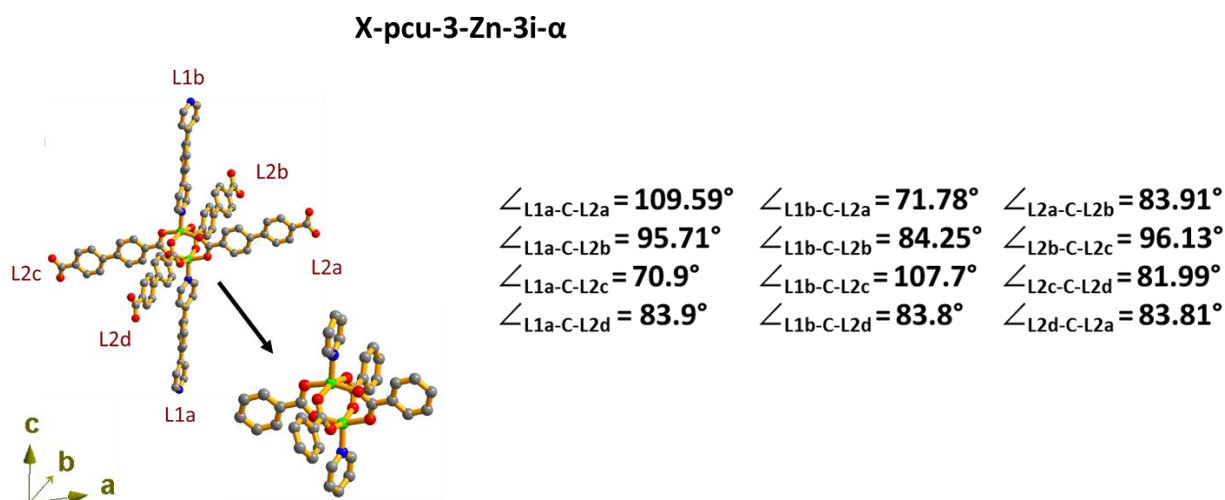
X-pcu-3-Zn-3i-α

$\angle_{L1a-C-L2a} = 109.59°$ $\angle_{L1b-C-L2a} = 71.78°$ $\angle_{L2a-C-L2b} = 83.91°$
$\angle_{L1a-C-L2b} = 95.71°$ $\angle_{L1b-C-L2b} = 84.25°$ $\angle_{L2b-C-L2c} = 96.13°$
$\angle_{L1a-C-L2c} = 70.9°$ $\angle_{L1b-C-L2c} = 107.7°$ $\angle_{L2c-C-L2d} = 81.99°$
$\angle_{L1a-C-L2d} = 83.9°$ $\angle_{L1b-C-L2d} = 83.8°$ $\angle_{L2d-C-L2a} = 83.81°$

fig. S11. Distortion of paddlewheel MBB and orientation of X-ligands in X-pcu-3-Zn-3i-α.

X-pcu-3-Zn-3i-β

$\angle_{L1a-C-L2a} = 90.45°$ $\angle_{L1b-C-L2a} = 89.54°$ $\angle_{L2a-C-L2b} = 46.83°$
$\angle_{L1a-C-L2b} = 103.13°$ $\angle_{L1b-C-L2b} = 76.86°$ $\angle_{L2b-C-L2c} = 132.16°$
$\angle_{L1a-C-L2c} = 89.54°$ $\angle_{L1b-C-L2c} = 90.45°$ $\angle_{L2c-C-L2d} = 46.83°$
$\angle_{L1a-C-L2d} = 76.86°$ $\angle_{L1b-C-L2d} = 103.13°$ $\angle_{L2d-C-L2a} = 132.16°$
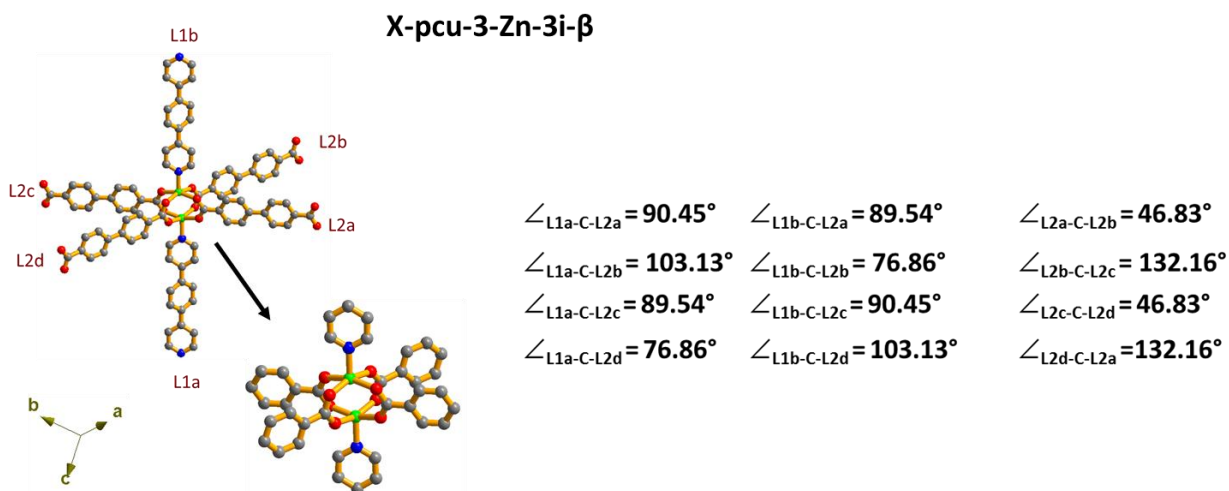
fig. S12. Distortion of paddlewheel MBB and orientation of X ligands in X-pcu-3-Zn-3i-β.

X-pcu-3-Zn-3i-γ
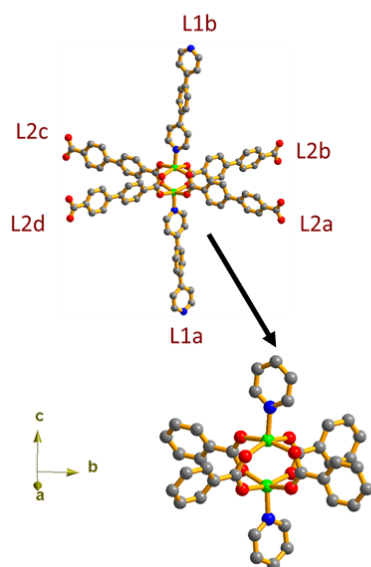
$\angle_{\text{L1a-C-L2a}} = 80.85°$ $\angle_{\text{L1b-C-L2a}} = 89.92°$ $\angle_{\text{L2a-C-L2b}} = 62.46°$

$\angle_{\text{L1a-C-L2b}} = 89.92°$ $\angle_{\text{L1b-C-L2b}} = 80.85°$ $\angle_{\text{L2b-C-L2c}} = 117.71°$

$\angle_{\text{L1a-C-L2c}} = 99.75°$ $\angle_{\text{L1b-C-L2c}} = 89.49°$ $\angle_{\text{L2c-C-L2d}} = 61.12°$

$\angle_{\text{L1a-C-L2d}} = 89.49°$ $\angle_{\text{L1b-C-L2d}} = 99.75°$ $\angle_{\text{L2d-C-L2a}} = 117.71°$

fig. S13. Distortion of paddlewheel MBB and orientation of X ligands in X-pcu-3-Zn-3i-γ.

Thermogravimetric analyses (TGA)
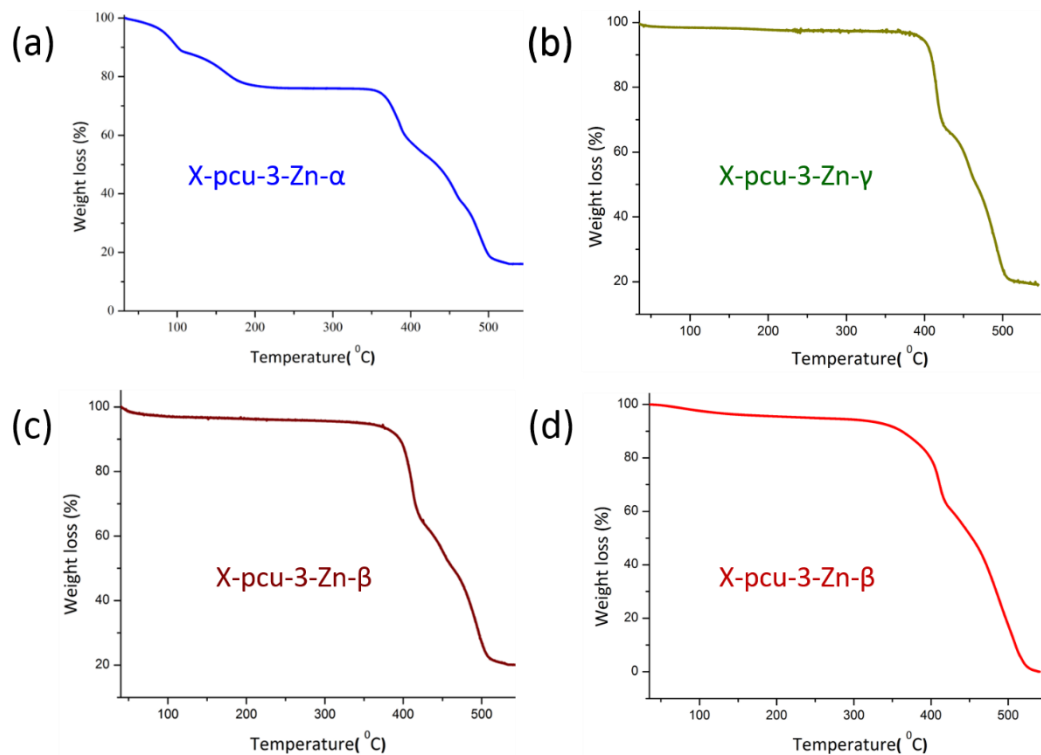
fig. S14. Thermogravimetric analysis (TGA) profiles. (A) as-synthesized **X-pcu-3-Zn-3i-α**, 24% weight loss corresponds to ~6 DMF. (B) **X-pcu-3-Zn-3i-γ** obtained after 195 K CO_2 sorption. (C) **X-pcu-3-Zn-3i-β** obtained after heating **X-pcu-3-Zn-3i-α** at 130 °C for 12 h. (D) **X-pcu-3-Zn-3i-β** obtained after washing (solvent exchange) **X-pcu-3-Zn-3i-α** with MeCN.

Molecular modelling
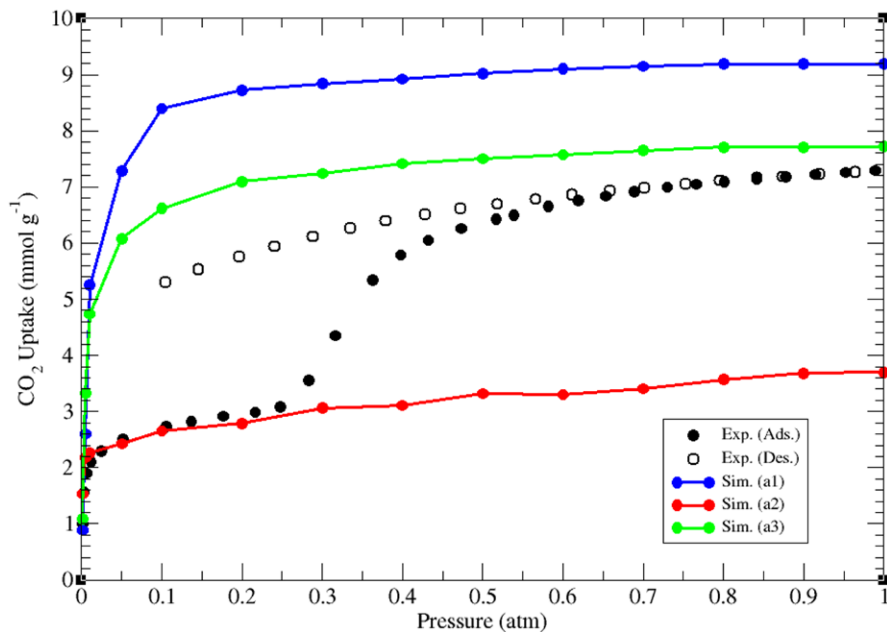
fig. S15. Comparison of modeling and experimental isotherm. Modelling experiments for both beta and gamma at 195K CO_2 is very well agreement with experimental gas sorption data.

(a)
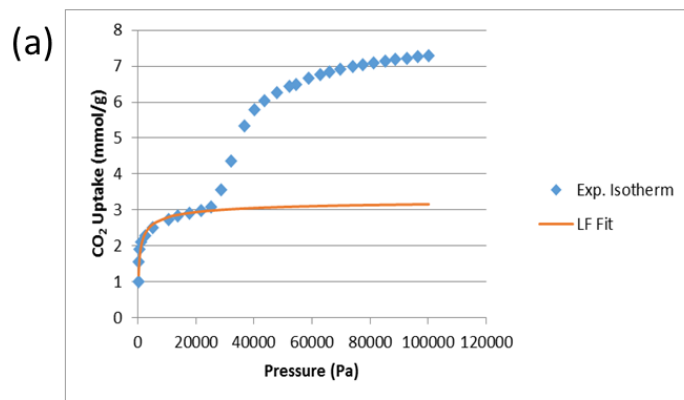
$N_{max1} =$	3.33240021	Avg. n =	2.355844545
$K_1 =$	0.03616024	TSS =	4.359192587
$n_1 =$	1.86179585	SSE =	0.089441069
		$R^2 =$	0.979482194

(b)
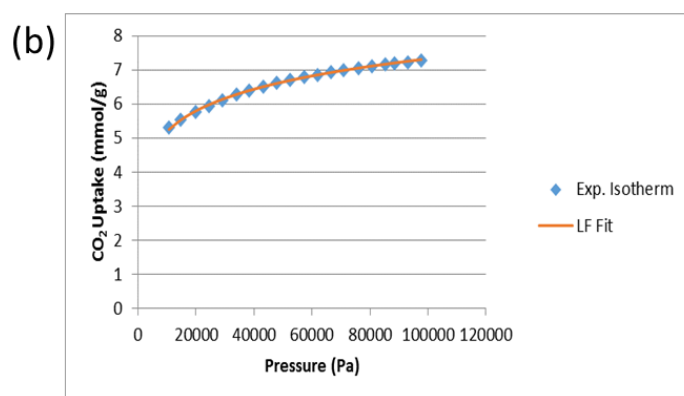
$N_{max2} =$	20.0923265	Avg. n =	6.587736
$K_2 =$	4.91E-02	TSS =	6.679401473
$n_2 =$	4.68798352	SSE =	0.007014548
		$R^2 =$	0.998949824

Estimation of free-energy difference ($0F$host) between X-pcu-3-Zn-3i-α and X-pcu-3-Zn-3i-β for CO_2 adsorption and desorption.

$\Delta F =$	31.75893195	kJ/mol

fig. S16. Free-energy difference. Langmuir-Freundlich (LF) fittings of the CO_2 adsorption (**A**) and desorption (**B**) isotherms for **X-pcu-3-Zn-3i-β** at 195 K.

A. Grand Canonical Monte Carlo

Simulations of CO_2 adsorption were performed in the three different phases (α, β, and γ) of **X-pcu-3-Zn-3i** using grand canonical Monte Carlo (GCMC) methods *(50)*. The single X-ray crystallographic structures that were obtained for all three phases herein were used for the parametrizations and simulations. All GCMC simulations were performed within the rigid crystal structures of the three individual phases. System cell dimension lengths of $2 \times 2 \times 1$, $2 \times 2 \times 2$, and $2 \times 1 \times 2$ were used for **X-pcu-3-Zn-3i-α**, **X-pcu-3-Zn-3i-β**, and **X-pcu-3-Zn-3i-γ**, respectively. A spherical cut-off distance corresponding to half the shortest system cell dimension length was used for the simulations in all three phases.

A five-site polarizable potential that was developed previously for CO_2 was used for the simulations in this work *(51)*. The total potential energy of the MOM–CO_2 system was calculated through the sum of the repulsion and dispersion, permanent electrostatic, and polarization energies. These were calculated using the Lennard-Jones 12–6 potential, partial charges with Ewald summation, and a Thole-Applequist type model *(52)*, respectively. The chemical potential for CO_2 was determined for a range of pressures and temperatures through the Peng-Robinson equation of state *(53)*. All simulations were performed using the Massively Parallel Monte Carlo (MPMC) code *(54)*. For all state points considered, the simulations consisted of 5.0×10^6 Monte Carlo steps to guarantee equilibration, followed by an additional 5.0×10^6 steps to sample the desired thermodynamic properties.

B. Parametrization

All atoms within the three different phases of **X-pcu-3-Zn-3i** were treated with Lennard-Jones 12–6 parameters, atomic point partial charges, and scalar point polarizabilities to model repulsion and dispersion, permanent electrostatic, and polarization interactions, respectively. The Lennard-Jones parameters (ε and σ) for all aromatic C, H, and N atoms were taken from the Optimized Potentials For Liquid Simulations – All Atom (OPLS-AA) force field *(55)*, while such parameters for Zn and O were taken from the Universal Force Field (UFF) *(56)*.

Examination of the crystal structure of the α, β, and γ phases of **X-pcu-3-Zn-3i** revealed 126, 42, and 42 atoms in chemically distinct environments, respectively (**Figures S17–S19**). The partial charges for the unique atoms in these phases were determined through electronic structure calculations on a variety of clusters that were extracted from the crystal structure of the respective phases. For these calculations, all light atoms (C, H, N, and O) were treated with the 6-31G* basis set, while the LANL2DZ ECP basis set *(57)* was used for Zn^{2+}. The NWChem *ab initio* software *(58)* was used to calculate the electrostatic potential surface for each fragment and the partial charges were subsequently fitted onto the atomic positions of the fragments using the CHELPG method *(59)*. For each chemically distinct atom, the partial charges were averaged between the fragments. The partial charges were then adjusted such that the total charge of the system was equal to zero. The final tabulated partial charges for each chemically distinct atom in **X-pcu-3-Zn-3i-α**, **X-pcu-3-Zn-3i-β**, and **X-pcu-3-Zn-3i-γ** are provided in **Tables S3**, **S5**, and **S7**, respectively. Note, the crystallographic distances between various chemically distinct atoms for the individual phases are provided in **Tables S4**, **S6**, and **S8**.

The exponential damping-type atomic point polarizabilities for all C, H, N, and O atoms were taken from a carefully parametrized set provided by the work of van Duijnen and Swart (C = 1.28860 $Å^3$, H = 0.41380 $Å^3$, N = 0.97157 $Å^3$, O = 0.85200 $Å^3$) *(60)*. The polarizability parameter for Zn^{2+} was determined in previous work (Zn^{2+} = 1.98870 $Å^3$) *(61)* and was used herein. These polarizability values were assigned to the nuclear centers of all atoms of the individual phases to model explicit polarization.

C. Density Functional Theory

The relative energies of the three different phases of **X-pcu-3-Zn-3i** were evaluated through periodic density functional theory (DFT) calculations that were implemented with the Vienna *ab initio* Simulation Package (VASP) *(62)*. These calculations were performed using the projector augmented wave (PAW) method with the Perdew–Burke–Ernzerhof (PBE) functional. In addition, dispersion effects were treated using the DFT-D3 correction method of Grimme *et al*.

Dispersion effects are expected to be important in the crystal structure of these phases since non-bonded portions of these structures are in close proximity to each other. The crystal structure of each phase of **X-pcu-3-Zn-3i** has varying number of atoms within its unit cell due to increasing or decreasing symmetry after each transition. Therefore, the calculated energies for the unit cell of the **β** and **γ** phases were subjected to a scalar (3 and 3/4, respectively) in order for these energies to be properly compared with that for the **α** phase.

The calculated energies for the three different phases of **X-pcu-3-Zn-3i** are displayed in **Table S7**. The calculations suggest that the **α** phase is the most stable phase of **X-pcu-3-Zn-3i** even though it is only representative of the material prior to activation. After activation, the material transitions to the **β** phase, which is the next most stable phase according to our calculations. After **X-pcu-3-Zn-3i-β** achieves CO_2 saturation, the material then transitions to the **γ** phase, which has the lowest energy of the three phases. Since the **α** phase is not accessed prior to or during CO_2 adsorption, it can be speculated that a prohibitive energy barrier exists between the **α** and **β** phases, which is catalyzed by the activation process to achieve the **β** phase, but not surmountable under successively applied conditions.
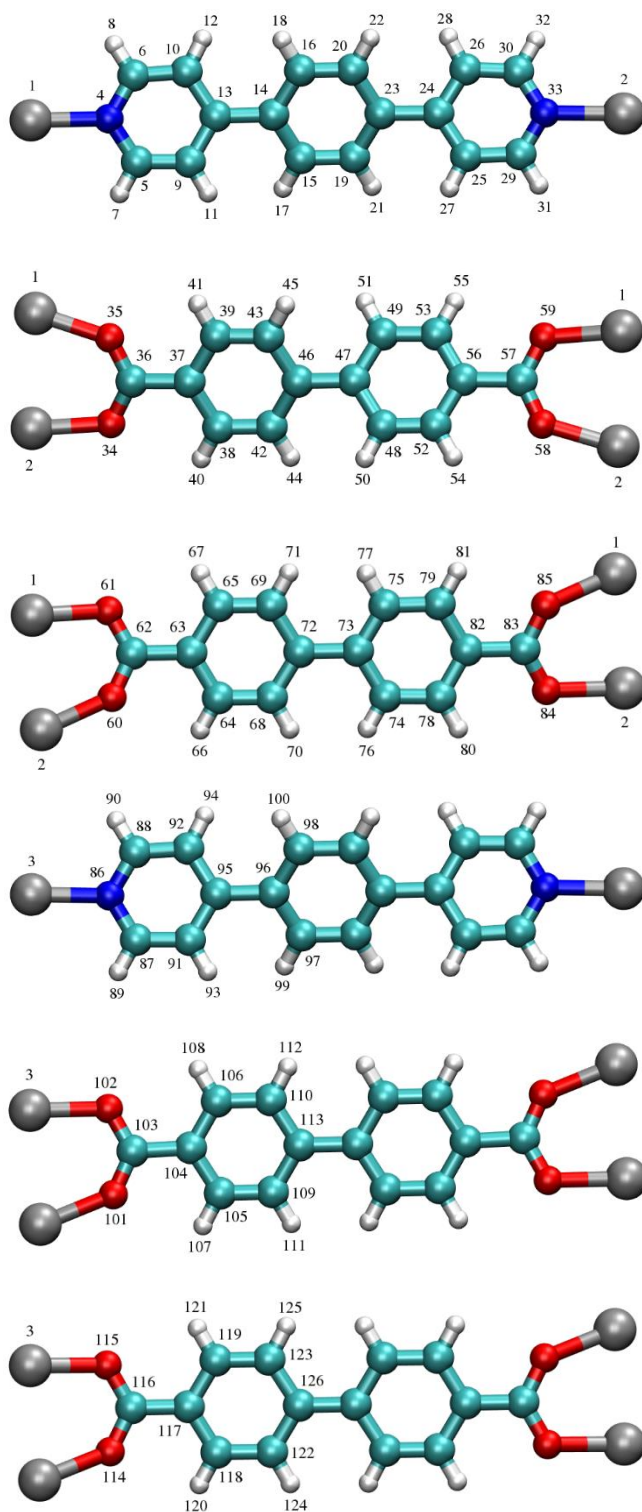
fig. S17. Chemically distinct atoms in X-pcu-3-Zn-3i-α. defining the numbering system corresponding to **Tables S3** and **S4**. Atom colors: C = cyan, H = white, N = blue, O = red, Zn = silver.
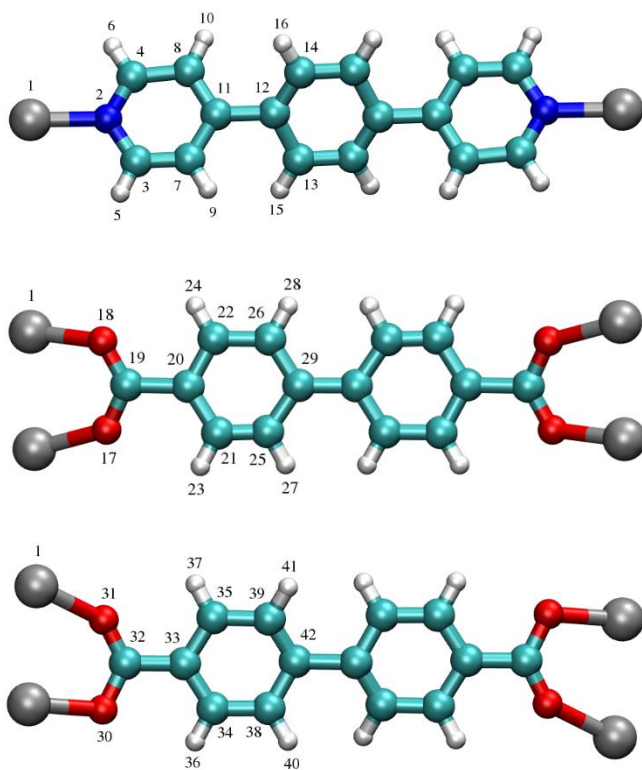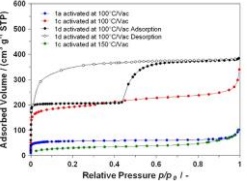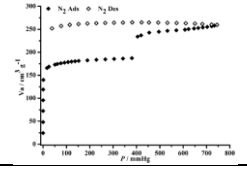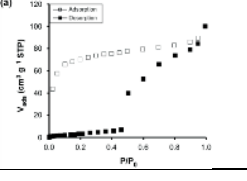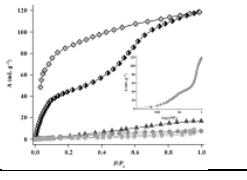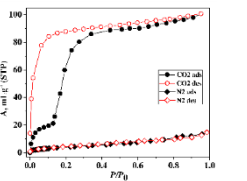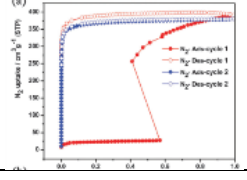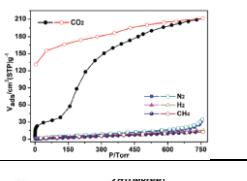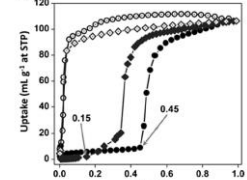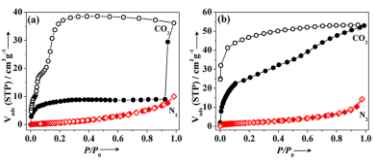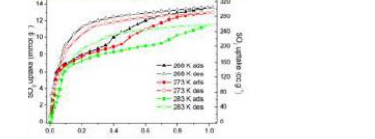
fig. S18. The chemically distinct atoms in X-pcu-3-Zn-3i-β. defining the numbering system corresponding to **Tables S5** and **S6**. Atom colors: C = cyan, H = white, N = blue, O = red, Zn = silver.
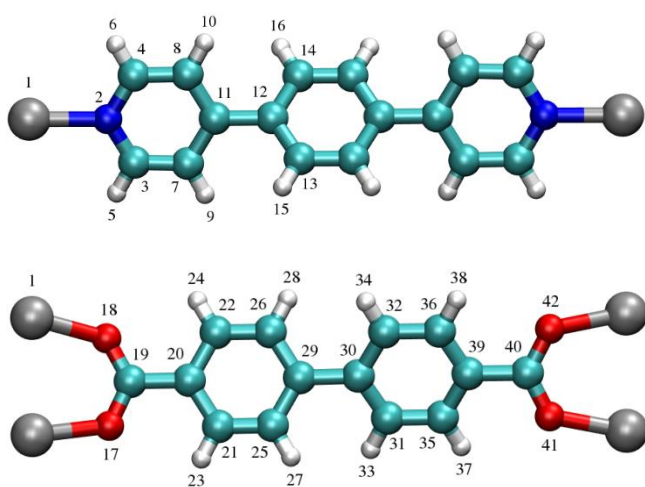
fig. S19. The chemically distinct atoms in X-pcu-3-Zn-3i-γ. Defining the numbering system corresponding to **Tables S7** and **S8**. Atom colors: C = cyan, H = white, N = blue, O = red, Zn = silver.

table S1. Examples of previously reported FMOMs with large hysteresis.

No.	Name of compound	isotherms	condition	references
1	[Cu$_4$(μ_4-O)(μ_2-OH)$_2$ (Me$_2$trz$p$ba)$_4$ or Cu-MOF (microcrystalline)		N$_2$@77K	*(41)*
2	[NH$_2$(CH$_3$)$_2$][Zn$_3$(4-Pca)$_3$(ade)]·10DMF·8H$_2$O		N$_2$@77K	*(42)*
3	{[Zn$_3$[μ4-bpdc)$_3${μ-bpdb)]·5DMF}$_n$		N$_2$@77K	*(43)*
4	[Cd(NH$_2$bdc)(bphz)$_{0.5}$]·DMF·H$_2$O}$_n$		CO$_2$@195K	*(44)*
5	{[Ni(1,3-adc)(bpp)]}$_n$		CO$_2$@195K	*(45)*
6	In(TCPBDA)(MeNH$_3$).6H$_2$O		N2@77K, Ar@87K, CO$_2$@195K	*(46)*
7	[CuL(Me$_2$NH)]·DMF·H$_2$O		CO$_2$@195K	*(47)*
8	f-MOF-1		CO$_2$@195K	*(37)*

9	[Cu-(bipy)$_{0.5}$(pyrdc)]and {[Cu-(bipy)$_{0.5}$(pyrdc)]		CO$_2$@195K	(48)
10	NOTT-202a		SO$_2$@268-283K	(49)

table S2. Crystal data and refinement parameters.

	X-pcu-3-Zn-3i-α	X-pcu-3-Zn-3i-β	X-pcu-3-Zn-3i-γ
Formula	$C_{84}H_{84}N_9O_{18}Zn_3$	$C_{44}H_{28}N_2O_8Zn_2$	$C_{44}H_{28}N_2O_8\ Zn_2$
F.W.	1703.77	421.73	421.73
T (K)	100(2)	100(2)	295(2)
Space group	P-1	P-1	$C/2c$
a (Å)	15.130(2)	9.4920(19)	16.375(3)
b (Å)	15.231(2)	10.295(2)	25.405(4)
c (Å)	18.253(3)	11.107(2)	14.007(2)
α (º)	84.956(5)	91.229(7)	90
β (º)	74.141(4)	101.020(7)	120.604(4)
γ (º)	83.962(5)	99.072(7)	90
V (Å^3)	4016.1(10)	1050.6(4)	5015.1(14)
Z	2	2	8
D_c (g cm^{-3})	1.046	1.333	1.117
μ (mm^{-1})	1.669	1.840	1.00
Data collected/unique	9445/8541	2940/2814	5781/4640
R_1 (>2σ)	0.0629	0.0596	0.0423
wR_2 (>2σ)	0.1788	0.1459	0.1123
GooF	1.045	1.100	1.169

table S3. Numerical labeling of atoms corresponds to fig. S17. The partial charges (in e^-) for the chemically distinct atoms in **X-pcu-3-Zn-3i-α**.

Atom	Label	q (e^-)
Zn	1	1.4172
Zn	2	1.3734
Zn	3	1.3788
N	4	−0.3763
C	5	0.1893
C	6	0.2534
H	7	0.1098
H	8	0.0918
C	9	−0.3322
C	10	−0.3468
H	11	0.1864
H	12	0.1818
C	13	0.2067
C	14	0.0992
C	15	−0.1550
C	16	−0.1799
H	17	0.1429
H	18	0.1555
C	19	−0.1873
C	20	−0.1639
H	21	0.1513
H	22	0.1485
C	23	0.0894
C	24	0.2692
C	25	−0.3838
C	26	−0.3771
H	27	0.1769
H	28	0.1803
C	29	0.2779
C	30	0.2388
H	31	0.0837

H	32	0.0778
N	33	−0.3635
O	34	−0.8132
O	35	−0.8370
C	36	0.9668
C	37	−0.2075
C	38	−0.0803
C	39	−0.0504
H	40	0.1320
H	41	0.1261
C	42	−0.2497
C	43	−0.2859
H	44	0.1410
H	45	0.1314
C	46	0.2091
C	47	0.2197
C	48	−0.2651
C	49	−0.2777
H	50	0.1381
H	51	0.1480
C	52	−0.0267
C	53	−0.0122
H	54	0.1192
H	55	0.1132
C	56	−0.2520
C	57	1.0055
O	58	−0.8300
O	59	−0.8147
O	60	−0.8347
O	61	−0.8359
C	62	0.9542
C	63	−0.1459
C	64	−0.1088
C	65	−0.0643

H	66	0.1354
H	67	0.1377
C	68	−0.1818
C	69	−0.2224
H	70	0.1293
H	71	0.1382
C	72	0.0848
C	73	0.1747
C	74	−0.2764
C	75	−0.2177
H	76	0.1523
H	77	0.1338
C	78	−0.0977
C	79	−0.1150
H	80	0.1338
H	81	0.1327
C	82	−0.1341
C	83	0.9767
O	84	−0.8061
O	85	−0.8476
N	86	−0.3661
C	87	0.2109
C	88	0.2394
H	89	0.1053
H	90	0.1064
C	91	−0.3729
C	92	−0.3835
H	93	0.1862
H	94	0.1943
C	95	0.2631
C	96	0.0481
C	97	−0.1650
C	98	−0.1817
H	99	0.1446

H	100	0.1531
O	101	−0.8190
O	102	−0.8332
C	103	0.9156
C	104	−0.1174
C	105	−0.1363
C	106	−0.0997
H	107	0.1336
H	108	0.1249
C	109	−0.2009
C	110	−0.2243
H	111	0.1324
H	112	0.1372
C	113	0.1640
O	114	−0.8391
O	115	−0.8371
C	116	0.9898
C	117	−0.1348
C	118	−0.0800
C	119	−0.0532
H	120	0.1254
H	121	0.1195
C	122	−0.2457
C	123	−0.2865
H	124	0.1416
H	125	0.1526
C	126	0.1313

table S4. The crystallographic distances (in Å) between various atoms in X-pcu-3-Zn-3i-α. Label of atoms correspond to **fig. S17**.

Atom Pair	Distance (Å)
1–4	2.02870
1–35	2.03068
1–59	2.04615
1–61	2.03281
1–85	2.05918
2–33	2.05153
2–34	2.04105
2–58	2.04570
2–60	2.02810
2–84	2.02658
3–86	2.03278
3–101	2.05332
3–102	2.04498
3–114	2.06882
3–115	2.03114
4–5	1.34929
4–6	1.30719
5–7	0.95074
6–8	0.94998
9–11	0.95016
9–13	1.37926
10–12	0.94911
10–13	1.39362
13–14	1.49203
14–15	1.40422
14–16	1.37752
15–17	0.95097
16–18	0.95054
19–21	0.94955
19–23	1.39157
20–22	0.95023

20–23	1.39034
23–24	1.49041
24–25	1.34527
24–26	1.34982
25–27	0.94855
26–28	0.94988
29–31	0.94933
29–33	1.25448
30–32	0.95039
30–33	1.30244
34–36	1.24086
35–36	1.25764
36–37	1.49542
37–38	1.41938
37–39	1.39962
38–40	0.94892
39–41	0.95091
42–44	0.95088
42–46	1.40304
43–45	0.95117
43–46	1.40311
46–47	1.46279
47–48	1.40608
47–49	1.40097
48–50	0.95006
49–51	0.94922
52–54	0.94948
52–56	1.38115
53–55	0.95004
53–56	1.37930
56–57	1.51441
57–58	1.25408
57–59	1.24350
60–62	1.25690

61–62	1.26022
62–63	1.50889
63–64	1.37596
63–65	1.40200
64–66	0.95097
65–67	0.94969
68–70	0.94971
68–72	1.38863
69–71	0.95032
69–72	1.41472
72–73	1.49177
73–74	1.38890
73–75	1.35833
74–76	0.94951
75–77	0.94961
78–80	0.95049
78–82	1.38629
79–81	0.94939
79–82	1.39366
82–83	1.49084
83–84	1.24096
83–85	1.26260
86–87	1.33612
86–88	1.32441
87–89	0.94927
88–90	0.94931
91–93	0.95003
91–95	1.38378
92–94	0.95016
92–95	1.39022
95–96	1.48077
96–97	1.38095
96–98	1.35974
97–99	0.94995

98–100	0.95004
101–103	1.23956
102–103	1.26429
103–104	1.50311
104–105	1.40161
104–106	1.38623
105–107	0.94975
106–108	0.94980
109–111	0.95140
109–113	1.40566
110–112	0.95023
110–113	1.39420
114–116	1.25910
115–116	1.26868
116–117	1.46397
117–118	1.38789
117–119	1.39343
118–120	0.94913
119–121	0.94852
122–124	0.95122
122–126	1.39184
123–125	0.94910
123–126	1.41910

table S5. The partial charges (in e^-) for the chemically distinct atoms in X-pcu-3-Zn-3i-β.
Label of atoms correspond to **fig. S18**.

Atom	Label	$q\ (e^-)$
Zn	1	1.4264
N	2	−0.3723
C	3	0.1963
C	4	0.2562
H	5	0.1173
H	6	0.0980
C	7	−0.3789
C	8	−0.4084
H	9	0.1777
H	10	0.2029
C	11	0.2888
C	12	0.0714
C	13	−0.2000
C	14	−0.1530
H	15	0.1680
H	16	0.1421
O	17	−0.8190
O	18	−0.8413
C	19	0.9474
C	20	−0.1174
C	21	−0.1015
C	22	−0.1454
H	23	0.1261
H	24	0.1442
C	25	−0.2141
C	26	−0.1966
H	27	0.1242
H	28	0.1285
C	29	0.1342
O	30	−0.8417

O	31	−0.8242
C	32	0.9310
C	33	−0.0645
C	34	−0.1359
C	35	−0.1488
H	36	0.1241
H	37	0.1192
C	38	−0.1599
C	39	−0.1305
H	40	0.1310
H	41	0.1292
C	42	0.0692

table S6. The crystallographic distances (in Å) between various atoms in X-pcu-3-Zn-3i-β. Label of atoms correspond to **fig. S18**.

Atom Pair	Distance (Å)
1–2	2.01601
1–17	2.05255
1–18	2.00208
1–30	2.06745
1–31	2.10029
2–3	1.34807
2–4	1.30802
3–5	0.94363
3–6	0.95336
7–9	0.94657
7–11	1.39635
8–10	0.94407
8–11	1.35556
11–12	1.50554
12–13	1.44932
12–14	1.29964
13–15	0.94593
14–16	0.94727
17–19	1.27175

18–19	1.26970
19–20	1.56064
20–21	1.40598
20–22	1.37627
21–23	0.94982
22–24	0.94230
25–27	0.95523
25–29	1.41385
26–28	0.94993
26–29	1.38569
30–32	1.30970
31–32	1.22990
32–33	1.48672
33–34	1.35348
33–35	1.37301
34–36	0.95008
35–37	0.95239
38–40	0.94880
38–42	1.36599
39–41	0.95511
39–42	1.28644

table S7. Numerical labeling of atoms corresponds to fig. S18. The partial charges (in e^-) for the chemically distinct atoms in **X-pcu-3-Zn-3i-γ**.

Atom	Label	q (e^-)
Zn	1	1.4050
N	2	–0.4173
C	3	0.2401
C	4	0.2350
H	5	0.1063
H	6	0.1111
C	7	–0.3804
C	8	–0.3598
H	9	0.1857
H	10	0.1799
C	11	0.2707
C	12	0.0783
C	13	–0.1645
C	14	–0.1789
H	15	0.1409
H	16	0.1494
O	17	–0.8213
O	18	–0.8299
C	19	0.9563
C	20	–0.1600
C	21	–0.1195
C	22	–0.0695
H	23	0.1419
H	24	0.1220
C	25	–0.2463
C	26	–0.2528
H	27	0.1434
H	28	0.1445
C	29	0.2001
C	30	0.2141
C	31	–0.2481

C	32	–0.2884
H	33	0.1323
H	34	0.1397
C	35	–0.0696
C	36	–0.0663
H	37	0.1164
H	38	0.1176
C	39	–0.1597
C	40	0.9892
O	41	–0.8365
O	42	–0.8511

table S8. Labels of atoms correspond to fig. S18. The crystallographic distances (in Å) between various atoms in **X-pcu-3-Zn-3i-γ**.

Atom Pair	Distance (Å)
1–2	2.03074
1–17	2.00319
1–18	2.06310
1–41	2.02543
1–42	2.06236
2–3	1.33747
2–4	1.34299
3–5	0.92949
4–6	0.92912
7–9	0.93033
7–11	1.38664
8–10	0.92959
8–11	1.36752
11–12	1.48041
12–13	1.38547
12–14	1.38425
13–15	0.93040
14–16	0.92988
17–19	1.25416

18–19	1.24624
19–20	1.49682
20–21	1.38722
20–22	1.39549
21–23	0.92894
22–24	0.93043
25–27	0.92940
25–29	1.39412
26–28	0.92926
26–29	1.38689
29–30	1.49019
30–31	1.34032
30–32	1.37172
31–33	0.92933
32–34	0.92978
35–37	0.92990
35–39	1.34987
36–38	0.93005
36–39	1.34618
39–40	1.50128
40–41	1.24788
40–42	1.25609

table S9. Calculated energies for three phases. Calculated energies (in eV) for the crystal structure of the three different phases (**α**, **β**, and **γ**) of **X-pcu-3-Zn-3i** as determined through periodic DFT calculations using VASP.

Phase	Energy (eV)
α	−1702.48
β	−1693.28
γ	−1689.73

The values shown for the **β** and **γ** phases are the result of multiplying the original calculated energy of the unit cell of these phases by 3 and 3/4, respectively.